ORIGINAL ARTICLE

Correspondence of Myocardial Strain with Torrent-Guasp's Theory. Contributions of New Echocardiographic Parameters

Correspondencia de la deformación miocárdica con la teoría de Torrent-Guasp. Aporte de nuevos parámetros ecocardiográficos

VICENTE MORA[1], ILDEFONSO ROLDÁN[1], ASSUMPCIÓ SAURÍ[1], RUBÉN FERNÁNDEZ-GALERA[1], MARTA MONTEAGUDO[1], ELENA ROMERO[1], CLAUDIA CABADÉS[1], JUAN A. COSÍN[2], JORGE C. TRAININI[MTSAC, 3], JORGE A. LOWENSTEIN[MTSAC, 4]

ABSTRACT

Background: Strain, assessed by speckle tracking echocardiography, may be used to evaluate left ventricular mechanics and could establish reference values together with new indices of myocardial function.
Objective: The aim of this study was to demonstrate the correspondence of echocardiographic strain values with Torrent-Guasp's single band theory.
Methods: A prospective observational study was conducted in 54 healthy volunteers. The three apical projections were used to determine longitudinal strain. Radial strain, circumferential strain and rotation were assessed in transverse planes at the level of the mitral valve, the papillary muscles and the apex.
Results: Mean age was 52±10.1 years. Global left ventricular longitudinal strain was -20.8%±2.4%. Post-systolic longitudinal strain mainly affects interventricular septal segments. Radial strain was 36.5%±10.7%, with basal values prevailing over apical ones, extending its duration to the early phase of diastole. Circumferential strain was -20.8%±3.8%, with larger values towards the apex. Twist was 18.4º±6º, torsion 2.2º±0.8º/cm and the torsion index (twist/mitral annular plane systolic excursion) 13.1º±4.4º/cm. The combined strain index includes the "strain product" (-387º±147º × %), and the "strain index" (-0.9º±0.3º/%) calculated as twist × longitudinal strain and twist/longitudinal strain, respectively.
Conclusions: New strain parameters may be useful in the study of ventricular mechanics. The anatomical arrangement described by the myocardial band theory is echocardiographically supported by the presence of larger radial strain at the basal-medial level (prevalence of transverse fibers), while the variable arrangement of oblique fibers are responsible for longitudinal strain, circumferential strain and ventricular torsion.

Key words: Echocardiography/methods- Ventricular Function, Left/physiology- Myocardial Contraction/physiology - Combined Strain Ratio

RESUMEN

Introducción: El strain, o deformación, evaluado mediante ecocardiografía speckle tracking, puede utilizarse para estudiar la mecánica del ventrículo izquierdo y permitiría establecer valores de referencia junto con nuevos índices de función miocárdica.
Objetivo: Demostrar la correspondencia de los valores ecocardiográficos con la teoría de la banda única de Torrent-Guasp.
Material y métodos: Estudio prospectivo observacional de 54 voluntarios sanos. Se utilizaron las tres proyecciones apicales para determinar el strain longitudinal. El strain radial, el strain circunferencial y la rotación se determinaron en planos transversales a nivel de la válvula mitral, los músculos papilares y el ápex.
Resultados: La edad media fue de 52,5±10,1 años. El strain longitudinal global del ventrículo izquierdo fue de -20,8% ±2,4%. Una deformación postsistólica en el strain longitudinal afecta fundamentalmente a segmentos del septo interventricular. El strain radial fue de 36,5% ±10,7%, con valores basales predominantes sobre los apicales, extendiendo su duración hasta la protodiástole. El strain circunferencial fue de -20,8% ±3,8%, con valores mayores hacia el ápex. El giro, o twist, fue de 18,4º ±6º, la torsión fue de 2,2º ±0,8º/cm y el índice de torsión (giro/excursión sistólica del anillo mitral) fue de 13,1º ±4,4º/cm. El índice combinado de deformación incluye el "producto de deformación" (-387º ±147º × %) y el "índice de deformación" (-0,9º ±0,3º/%), calculados como giro × strain longitudinal y giro/strain longitudinal, respectivamente.
Conclusiones: Nuevos parámetros de deformación pueden ser útiles en el estudio de la mecánica ventricular. La disposición anatómica descripta por la teoría de la banda miocárdica se ve apoyada ecocardiográficamente por la presencia de mayor strain radial a nivel basal-medial (predominio de fibras transversales), mientras que la disposición variable de las fibras oblicuas son las responsables del strain longitudinal, el strain circunferencial y la torsión ventricular.

Palabras clave: Ecocardiografía/métodos - Función ventricular izquierda/fisiología - Contracción miocárdica - Parámetro combinado de deformación

Rev Argent Cardiol 2016;84:541-549. http://dx.doi.org/10.7775/rac.v84.i6.9656

Received: 09/21/2016 – *Accepted:* 10/27/2016

Address for reprints: Vicente Vicente Mora Llabata - Servicio de Cardiología. Hospital Universitario Doctor Peset - Avda. Gaspar Aguilar 90. 46017. Valencia, España - Tel. 96 1622589. Fax 96 1622589 - e-mail: vmoral@comv.es

[MTSAC] Full Member of the Argentine Society of Cardiology
[1] Department of Cardiology - Hospital Universitario Doctor Peset. Valencia, España
[2] Experimental Cardiology Unit - Hospital Universitario La Fe Research Center. Valencia. Spain.
[3] Hospital Presidente Perón. Buenos Aires, Argentina. Fundación y Centro de Ingeniería Biomédica y Tecnologías Sanitarias. Madrid, Spain
[4] Cardiac Diagnostic Unit, Investigaciones Médicas de Buenos Aires. Argentina

Abbreviations

CS	Circumferential strain
ECG	Electrocardiogram
LS	Longitudinal strain
LV	Left Ventricular
MAPSE	Mitral annular plane systolic excursion
NT-ProBNP	N-terminal pro B-type natriuretic peptide
PSS	Post-systolic strain
RS	Radial Strain
STEc	Speckle Tracking Echocardiography

INTRODUCTION

Left ventricular (LV) function is the result of contraction and relaxation of a complex myocardial fiber architecture producing changes in the shape and size of the left ventricle. (1, 2)

Strain, obtained from speckle tracking echocardiography (STEc) allows the quantification of regional myocardial function. (3, 4) Speckle tracking echocardiography enables the estimation of myocardial longitudinal strain (LS), radial strain (RS) and circumferential strain (CS), independently of the image acquisition angle, and evaluates LV rotational mechanics. (5, 6) Its accuracy has been validated with sonomicrometry and magnetic resonance imaging. (7-9)

Two of the most controversial approaches to describe cardiac myofibrillar architecture and function are the myocardial network proposed by Anderson et al. (10, 11) and Torrent-Guasp's ventricular myocardial band. (12, 13) The myocardial network model postulates a longitudinal and radial myocyte arrangement, with varying angles according to myocardial depth. Torrent-Guasp et al. (12-14) described the helical myofiber orientation as a single double helix myocardial band that forms two loops, a basal transverse loop and an apical oblique loop with a descending and an ascending component. The transverse fibers of the basal loop enclose the apical loop including the upper two-thirds and to a lesser degree the inferior or apical third (Figure 1).

The aim of this study was to obtain reference strain values using two-dimensional STEc, together with new indices of myocardial function, and to analyze the correspondence of strain with the muscular arrangement described by Torrent-Guasp's myocardial band theory.

METHODS

Study population

An observational, prospective study was designed including 54 healthy volunteers. Inclusion criteria were: age >18 years, absence of cardiovascular disease, and normal physical and electrocardiographic examinations. Exclusion criteria were sports training, pregnancy and presence of cardiovascular risk factors.

Echocardiography

A Vivid E9 ultrasound system (GE, Healthcare Medical Systems, Norway) equipped with 2.5 MHz tranducer was used. Two-dimensional projections were obtained from the apical

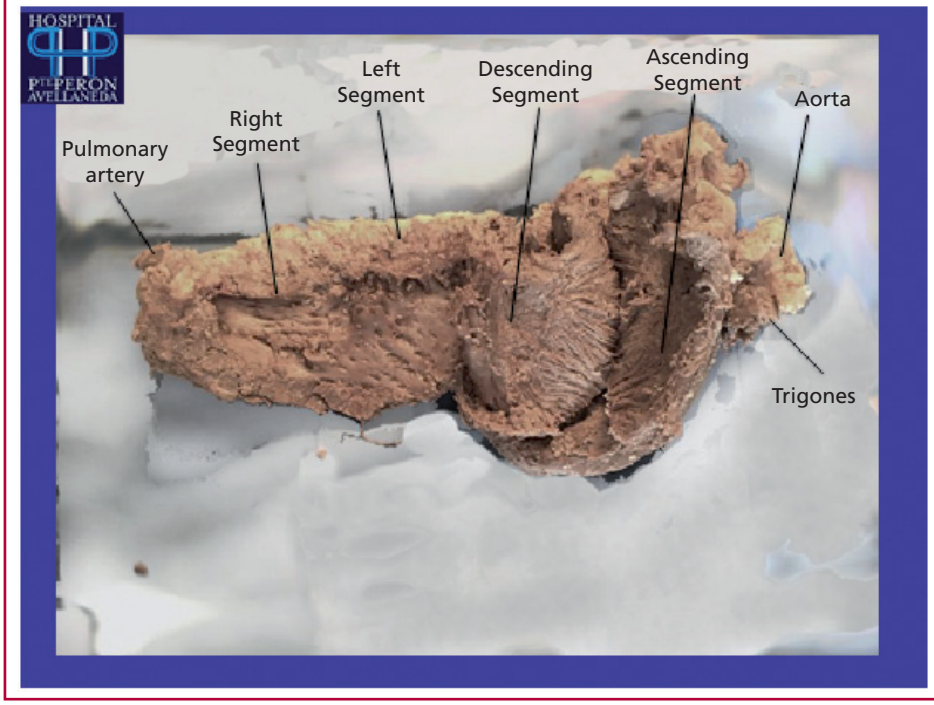

Fig. 1. The figure shows the descending segment fibers. A cleavage plane was obtained in the ascending segment to observe how the fibers spiral (from horizontal to vertical) to achieve the mechanical effect of ventricular torsion. Dissection performed by Drs. Jorge and Alejandro Trainini.

plane (four and two chamber, and long axis views) to calculate LS, and parasternal projections (transverse projections at the mitral valve, papillary muscle and apical levels) to calculate RS, CS and rotation parameters. All images were obtained at a frequency of 50-80 frames/second. The moment of aortic valve closure was determined in the long-axis apical projection. All studies were transferred to a workstation for analysis with a software program (EchoPAC GE Healthcare software version 112.0.0).

The LV endocardial border was traced slightly inside the myocardium. Then, a larger second concentric circle was automatically generated near the epicardium to include all the myocardium. The program automatically divided each projection into six equal segments and performed frame by frame speckle tracking, providing automatized tracking confirmation (verified by the operator) and generating strain values, expressed as percentage.

Rotation is the transverse angular shift of a myocardial segment around the LV longitudinal axis. (15) Counterclockwise apical systolic rotation is expressed in degrees with positive values seen from the apex, and clockwise basal rotation with negative values. Twist is the net difference between apical and basal rotation.

The occurrence and type of post-systolic strain (PSS) was analyzed from the LS (Figure 2A). Systolic and post-systolic "strain duration" was estimated as the time elapsed from QRS onset in the ECG to maximum LS, and the difference between both. (16)

The distance between the base and the apex was assessed in end-diastole at QRS onset. Left ventricular longitudinal shortening was estimated from the mitral annular plane systolic excursion (MAPSE) in the four-chamber apical plane by placing the M-mode pointer at the septal and lateral annular level, and averaging both values. (17)

The following parameters were evaluated to assess LV myocardial function:

a) Torsion: Twist/apex-base distance (degrees/cm).
b) Torsion Index: Twist/MAPSE (degrees/cm).
c) Combined strain parameter:
- Strain product: Twist × LS (degrees × %).
- Strain index: Twist/LS (degrees/LS).

Statistical analysis

Continuous variables are expressed as mean and standard deviation. Strain values between men and women and between regions were compared using Student's t test and analysis of variance (ANOVA) as appropriate. A p value <0.05 was considered as statistically significant.

The intraclass correlation coefficient (ICC) was used to evaluate intraobserver and interobserver reproducibility of continuous variables, according to a random sample of 10 cases, with masking and measurements performed at different moments. Graphical representation was analyzed using the Bland-Altman method. The Saphiro-Wilk test was used to assess normal parameter distribution.

Statistical analyses were performed using IBM SPSS Statistics v.19.0.0329 software package.

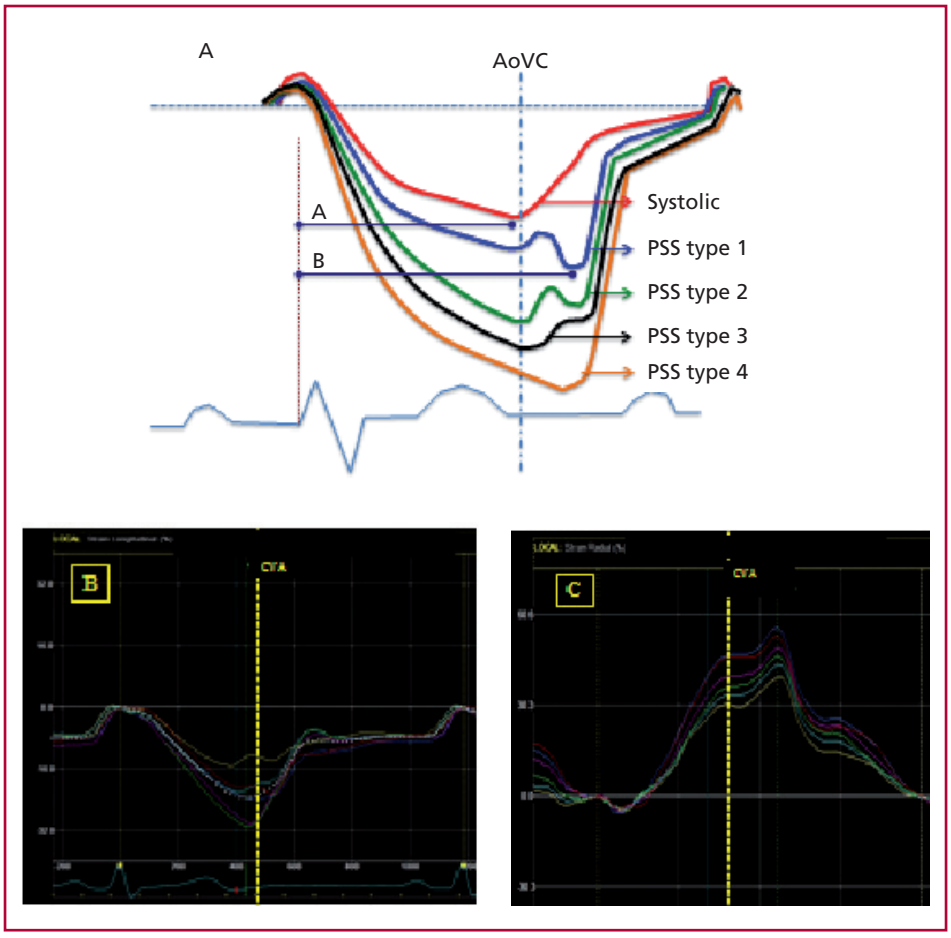

Fig. 2. A: Representation of morphologic types of longitudinal strain observed in healthy subjects (mentioning only morphology, independently of amplitude). a: Duration of systolic strain. b: Duration of post-systolic strain. B. Interventricular septum medial (light blue) and basal (yellow) post-systolic strain and basolateral post-systolic strain (red).C. Basal radial strain. See color image in the website. AoVC: Aortic valve closure. PSS: Post-systolic strain.

Ethical considerations

The study was approved by the hospital Ethics Committee and written informed consent was obtained from all study participants.

RESULTS

Table 1 details population characteristics. Global LV LS amplitude was -20.8%±2.4% (Table 2), with regional values that increase from the LV base to the apex. A more frequent PSS was observed in the interventricular septal segments, and in the basal segments of the adjacent anterior and inferior walls (Figures 2B and 3). Mean systolic and post-systolic strain duration were 359±30 ms and 447±28 ms, respectively, with a difference between both of 88±7.1 ms (see Table 2).

Radial strain was predominantly found at basal and medial levels compared with apical levels (see Table 2). Its duration extends to the first phase of diastole, being more evident at the basal level (Figure 2C). Global LV CS showed progressively larger amplitude values from the base to the apex (see Table 2).

Left ventricular rotation, twist and torsion

At the beginning of rotation, a movement contrary to the regional dominant one is characteristic both at basal and apical levels (Figure 4). Mean apical and basal rotation values at the moment of maximum LV systolic twist are shown in Table 2. Net twist was 18.4º ±6º, and maximum torsion 2.2º ±0.8º/cm.

The torsion index, calculated as the ratio between twist and MAPSE was 13º.1±4.4º/cm.

The combined strain parameter is used as a more complete overall and sensitive estimation of myocardial function (strain product: -387º±147º × %), and the type of its alteration (strain index: -0.9º±0.3º/%) (see Table 2). Intraobserver and interobserver variability was suitable (Table 3), with intraclass correlation coefficients >0.75. Compared with subjects <50 years, in those with ages ≥50 years, twist (19.5º±6.1º vs. 15.6º±5.0º; p=0.03), torsion (2.4º±0.8º vs. 1.7º±0.6º; p=0.01), and the torsion index (14.2º±4.5º vs. 10.6º±3.0º; p=0.001) were higher. The strain product showed no differences with age, whereas in subjects aged ≥50 years the strain index was greater (-0.9º±0.3º vs. 0.7º±0.1º; p=0.01). Gender differences in strain parameters and rotational mechanics are shown in Table 2.

DISCUSSION

Left ventricular myocardial strain and rotational mechanics

We present LV strain and rotational mechanics values in an adult healthy population, together with new parameters that can be useful in the evaluation of LV function.

A predominant RS was observed in the basal region and a dominant CS in the apical region, whereas LS showed more uniform regional values increasing towards the apex. According to a recent meta-analysis (18) including 2,597 subjects (age 47±11 years; 51% men), normal LS values range between -15.9% and -22.1%, CS between -20.9% and -27.8%, and RS between 35.1% and 59%, with larger values of LS and CR increasing towards the apex.

The twist values agree with results reported by Kocabay et al., (2) lower in 36-55-year old subjects (18.9º±7.3º) compared with those observed in persons aged between 56-80-years (23º±8º). Both LV rotation, especially apical, as LV torsion are determinant factors of LV function, and usually increase with age, (18, 19) as reflected by our series. Strain, torsion and the torsion index were similar in both sexes (see Table 2), though there is still controversy in this regard. (18-20)

Torsion is calculated as the ratio of twist/apex-base distance at end-diastole, though the exact measurement of the denominator by two-dimensional-echo can be inaccurate to define the apical endocardium. (21) Physiologically, the torsion index (twist/MAPSE) may be more realistic, as both parameters express the active movements produced simultaneously during systole "squeezing" the left ventricle.

Table 1. Population characteristics (n=54), divided by sex

	Total (n=54)	Men (n=32)	Women (n=22)	p
Age	52.5±10.1	53.0±8.9	51.7±11.8	0.65
Body surface area	1.8±0.2	1.9±0.1	1.6±0.1	0.001
Heart rate	63±10	60±11	66±9	0.04
Systolic blood pressure, mm Hg	127±15	130±14	122±15	0.05
Left atrium, cm2	16±3	17±3	14±2	0.01
Diastolic left ventricle, mm	46.8±4.5	48.6±4.6	44.4±2.9	0.001
Left ventricular mass	172.6±50.2	192.1±54.0	145.1±26.7	0.001
LVESV, ml	93.1±30.4	105.5±28.1	75.0±24.3	0.001
LVEDV, ml	29.8±11.7	34.6±11.5	22.7±8.2	0.001
LVEF, %	68.2±5.1	67.4±5.3	69.5±5.3	0.13

LVESV: Left ventricular end-systolic volume. LVEDV: Left ventricular end-diastolic volume. LVEF: Left ventricular ejection fraction.

Table 2. Longitudinal, radial and circumferential strain values and rotation parameters in the total population and divided by sex

	Total (n=54)	Men (n=32)	Women (n=22)	p
Longitudinal strain				
Basal	-19.6±2.4	-19.2±2.3	-20.2±2.5	0.11
Medial	-21.2±2.4	-20.7±2.1	-21.9±2.7	0.08
Apical	-21.9±3.6	-21.2±3.5	-22.9±3.5	0.09
Global	-20.8±2.4	-20.3±2.2	-21.6±2.6	0.06
Radial strain				
Basal	44.2±18.5	44.5±22.9	43.8±18.1	0.90
Medial	41.8±16.1	42.4±18.5	41.1±12.2	0.77
Apical	23.5±16.1	23.5±12,6	23.5±20.4	0.99
Global	**36.5±10.7**	**36.8±10.7**	**36.1±11.1**	**0.82**
Circumferential strain				
Basal	-16.8±3.5	-16.5±3.5	-17.3±3.7	0.47
Medial	-19.8±5.0	-20.5±5.2	-18.9±4.7	0.26
Apical	-25.6±6.6	-25.7±7.6	-25.5±5.2	0.89
Global	**-20.8±3.8**	**-20.9±3.9**	**-20.5±20.8**	**0.73**
MAPSE, cm	1.4±0,1	1.4±0.1	1.3±0.1	0.11
SSD, ms	359±30	352±30	367±29	0.08
PSSD, ms	447±28	442±22	453±33	0.17
PSSD-SSD, ms	88.2±7.1	90.2±9.7	85.9±2.5	0.10
Apical rotation, degrees	12.5±4.6	12.6±4.2	12.5±5.3	0.95
Basal rotation, degrees	-5.9±3.7	-5.5±3.7	-6.5±3.6	0.31
Twist, degrees	18.4±6.0	18.0±5.5	18.9±6.8	0.59
Torsion, degrees/cm	2.2±0.8	2.0±0.7	2.4±0.9	0.08
Torsion index, degrees/cm	13.1±4.4	12.6±4.2	13.9±4.6	0.30
Combined strain parameter				
Strain product, degrees × %	-387±147	-367±120	-416±178	0.23
Strain index, degrees/%	-0.9±0.3	0.9±0.3	0.9±0.3	0.80

MAPSE: Mitral annular plane systolic excursion. SSD: Systolic strain duration. PSSD: Post-systolic strain duration.

Table 3. Intraobserver and interobserver variability

Intraobserver	Intraclass correlation coefficient (95% CI)	p
Global longitudinal strain	0.86 (0.53-0.96)	<0.001
Twist	0.94 (0.65-0.98)	<0.001
Torsion	0.96 (0.84-0.99)	<0.001
Torsion index	0.93 (0.63-0.98)	<0.001
Strain product	0.97 (0.82-0.99)	<0.001
Strain index	0.85 (0.52-0.96)	<0.001
Interobserver		
Global longitudinal strain	0.87 (0.58-0.96)	<0.001
Twist	0.85 (0.53-0.96)	<0.001
Torsion	0.87 (0.59-0.96)	<0.001
Torsion index	0.80 (0.41-0.94)	<0.001
Strain product	0.90 (0.65-0.97)	<0.001
Strain index	0.77 (0.31-0.94)	0.003

It is important to differentiate myocardial function from ventricular function, the latter being a consequence of the former. Longitudinal strain and twist have been revealed as sensitive parameters to assess myocardial function before translating into ventricular dysfunction. (22) Normal LS values have been established, (23) whereas twist values are less typified. We postulate using a "combined strain parameter" to evaluate LV function, so that the "strain product (twist × LS)" accounts for myocardial function and the "strain index (twist/LS)" the predominant type of alteration. A "normal" product would translate into globally preserved LV function, either by normality of both parameters or by the compensation provided between them ("pseudonormal" product). A decreased "strain product" may be due to decreased LS, twist, or both, and would be characterized by the value of the "strain index" (high, low or normal index, respectively). Thus, this "combined strain parameter" may

help to promptly detect, identify the type and monitor the myocardial impairment produced in some cardiomyopathies or oncological treatments.

Mornos et al. (24) observed the negative correlation of the LV torsion × LS product, similar to the "strain product", with NT-proBNP values in patients with dilated cardiomyopathy. Its isolated assessment may conceal a pseudonormal value. However, the "combined strain parameter" (product and index) would provide more complete information of myocardial function.

Relationship with Torrent-Guasp's myocardial band theory

The structural muscular distribution of the left ventricle according to the data provided by strain is in agreement with Torent Guasp's proposal (12-14) and is useful to understand how endocardial to epicardial activation explains LV torsion.

Muscular arrangement

The myocardial muscle mass mainly concentrates at the LV medio-basal level where basal and apical loop fibers meet. This supports that the maximum deformation amplitude obtained with RS occurs at this level, also extending its duration to occupy the isovolumic relaxation period and part of early diastole (see Table 2 and Figure 2C). Longitudinal strain, chiefly related with the action of endocardial descending fibers increases towards the apex. These fibers progressively acquire a more oblique arrangement until they reach the apex (translating into greater longitudinal strain), where they reverse their arrangement forming a loop before adopting an ascending direction (see Figure 1). At the apical level, the CS is of greater amplitude (see Table 2), enabling apical rotation. At the basal level, the apical loop fibers also adopt an oblique arrangement aiding basal rotation, though of lower amplitude (see Table 2 and Figure 4).

Longitudinal strain shows a characteristic PSS in some myocardial segments when diastolic recovery has already started (see Figure 2A and B). This is mainly observed in septal segments and in adjacent anterior and inferior basal segments (see Figure 3), corresponding in time with the final part of RS, and similarly to it, it is produced in the first phase of diastole. This means that contractile activity is recorded in the first phase of diastole, when ventricular relaxation has already started. The segments with post-systolic LS correspond with the anatomical position of the ascending band described by Torrent-Guasp, presenting a more epicardial arrangement. The difference between systolic and post-systolic strain duration was 88.2±7.1 ms, similar to the QRS duration in our population of healthy subjects without intraventricular conduction abnormalities, and would be explained by the late activation of the myocardial band ascending epicardial fibers involved in early diastolic ventricular suction, as pointed out by Trainini et al. (25) from electrophysiological studies. Using three-dimensional electroanatomic cartographic mapping they describe the initiation of LV activation in the interventricular septum endocardium towards the epicardium. They detected that chamber endocardial activation ends well before the end of the QRS, so that the latest activation would correspond to the activation of the distal

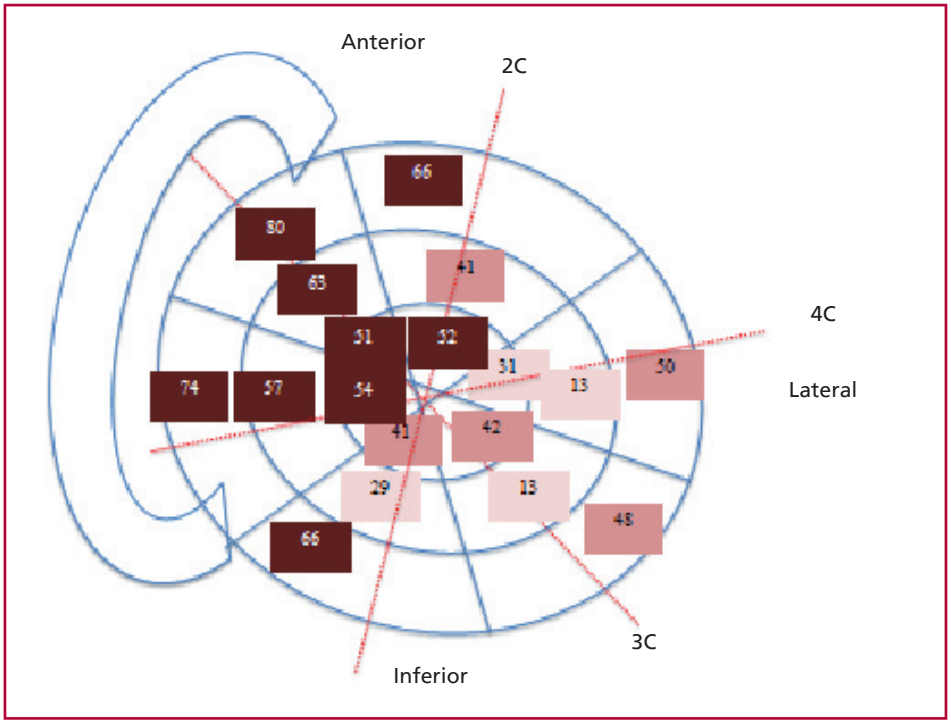

Fig. 3. Bull's-eye representation of frequency (%) in the post-systolic strain localization according to the segments.

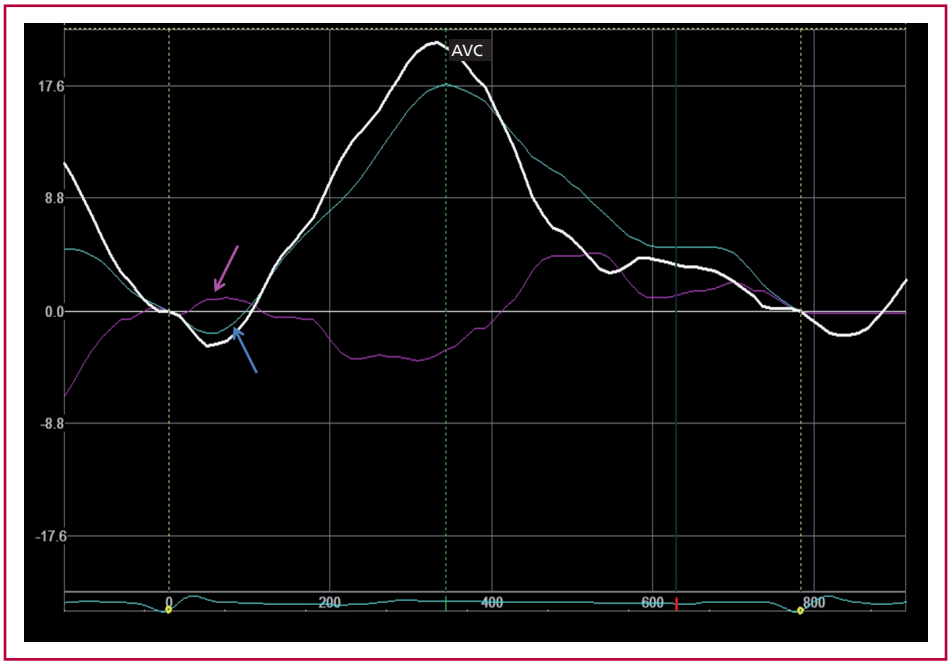

Fig. 4. Basal rotation (*pink line*), apical rotation (*blue line*) and twist (*white line*). Basal initial (*pink arrow*) and apical (*blue arrow*) systolic rotation in opposite direction to the regional predominant one. AVC: Aortic valve closure (*vertical dotted line*). See color image in the website.

portion of the ascending fibers, explaining the persistence of contraction during the isovolumic phase of diastole, basis of the ventricular suction mechanism. This phenomenon corresponds in time with the duration of PSS perceived with LS at this level, and with the prolongation of LS and RS to the first phase of diastole observed in our study.

Cosin et al. (26) show experimentally, using intramyocardial piezoelectric crystals, that during the LV isovolumic relaxation phase, the ascending segment of the apical loop is contracting. The infiltration of the ascending segment with formaldehyde prolongs the duration of the isovolumic relaxation phase and the capacity to reduce intraventricular pressure at the beginning of diastole. The localization described for this ascending segment corresponds with the anteroseptal segments where post-systolic deformation is observed with strain.

Studies performed by Poveda et al. (27), through the experimental analysis of tractographic reconstructions with magnetic resonance imaging reveal a continuous helicoidal organization of myocardial fibers in accordance with the single ventricular band model.

Contractile activation and torsion mechanics

The myocardial band theory sustains the understanding of an initial subendocardial activation towards the epicardium contracting in opposite directions, and is capable of explaining the torsion movement by its double helix arrangement. Systolic LS and CS translate into myocardial thickening registered by RS with positive values due to this myofibrillar arrangement. If RS were "active" by muscle shortening of fibers arranged radially, it should be coded with negative values by STEc, and this does not occur in healthy subjects. Radial strain appears then as a consequence of LS and CS.

The transmural propagation of electrical activation results in sequential shortening of subendocardial to subepicardial fibers. (28-30) The subendocardial descending fibers of the apical loop would initiate contraction, subsequently propagating by transverse and ascending fibers progressively arranged in opposite directions. The greater radius of the subepicardial region dominates the direction of rotation. (28)

During isovolumic contraction, the LV apex shows a brief clockwise rotation that quickly reverses and transforms into counterclockwise rotation during LV ejection. (30, 31) This movement reverses (in clockwise direction) during isovolumic relaxation and early diastole. The opposite takes place at the base of the left ventricle, but at a lower magnitude. Strain is able to reveal this characteristic systolic rotation (see Figure 4).

The participation of myocardial elastic proteins is important in this process through their mechanosensory function. (32) Titin, through conformational changes, acts as a pressure sensor during contraction and as a distension sensor during relaxation. (32-35) The rotation of subendocardial fibers twist the muscle matrix resulting in storage of potential energy that is subsequently used for diastolic recoil. (28-30) The initial phase of diastole appears linked both to the action of myocardial elastic proteins as to the final contraction of Torrent-Guasp's apical loop ascending fibers acting successively and jointly. Modifications produced both in titin structure as well as at the anatomical level of the ascending fibers (26) translate into abnormal LV filling pressures. We can see that anatomical, (12-14) cartographic, (25) sonomicrometry, (26) magnetic

resonance, (27) molecular (34-37) data, and those obtained with STEc in the present work support the arrangement of Torrent-Guasp's myocardial band.

Limitations

Routine application of myocardial strain in clinical practice requires the definition of normal ranges. New parameters should demonstrate their usefulness in different cardiac diseases.

A wide variety of parameters may potentially influence strain measurement, including patient anthropometric, hemodynamic and cardiac aspects and differences in the software used to calculate strain. However, we do not think that these limitations interfere with the interpretation of the muscle band theory. The analysis by layer (endocardial, myocardial and epicardial) which might provide additional data has not been performed.

CONCLUSIONS

We postulate new additional parameters to study ventricular mechanics by means of STEc, which might enable the understanding of cardiac physiology and should demonstrate their usefulness in cardiac diseases.

The data obtained from the ventricular myocardium using STEc echocardiographically support the myofibrillar arrangement described in the myocardial band theory, capable of explaining the ventricular shortening and torsion phenomena, and uphold the participation of active muscle contraction during the first part of diastole.

Conflicts of interest

Dr. Jorge Lowenstein has received medical fees for conferences on behalf of General Electric. The rest of the authors declare no conflicts of interest. (See authors' conflicts of interest forms in the website/Supplementary material).

REFERENCES

1. Zaca V, Ballo P, Galderisi M, Mondillo S. Echocardiography in the assessment of left ventricular longitudinal systolic function: current methodology and clinical applications. Heart Fail Rev 2010;15:23-37. http://doi.org/cztpfd

2. Kocabay G, Muraru D, Peluso D, Cucchini U, Mihaila S, Padayattil-Jose S, et al. Mecánica ventricular izquierda normal mediante ecocardiografía speckle tracking bidimensional. Valores de referencia para adultos sanos. Rev Esp Cardiol 2014;67:651-8. http://doi.org/f2rd8v

3. D'Hooge J, Heimdal A, Jamal F, Kukulski T, Bijnens B, Rademakers F. Regional strain and strain rate measurements by cardiac ultrasound: principles, implementation and limitations. Eur J Echocardiogr 2000;1:154-70. http://doi.org/fkfd2h

4. Gorcsan J, Tanaka H. Echocardiographic assessment of myocardial strain. J Am Coll Cardiol 2011;58:1401-13. http://doi.org/frrwbp

5. Lang RM, Badano LP, Mor-Avi V, Afialo J, Armstrong A, Ernande L, et al. Recommendations for cardiac chamber quantification by echocardiography in adults: an update from the American Society of Echocardiography and the European Association of Cardiovascular Imaging. J Am Soc Echocardiogr 2015;28.1-39.e14. http://doi.org/bhj5

6. Takeuchi M, Nishikage T, Nakai H, Kokumai M, Otani S, Lang RM. The assessment of left ventricular twist in anterior wall myocardial infarction using two-dimensional speckle tracking imaging. J Am Soc Echocardiogr 2007;20:36-44. http://doi.org/cdj7cw

7. Notomi Y, Setser RM, Shiota T, Martin-Miklovic MG, Weaver JA, Popovic ZB, et al. Measurement of ventricular torsion by two-dimensional ultrasound speckle tracking imaging. J Am Coll Cardiol 2005;45:2034-41. http://doi.org/bwgh3f

8. Helle-Valle T, Crosby J, Edvardsen T, Lvseggen E, Amundsen BH, Smith HJ, et al. New noninvasive method for assessment of left ventricular rotation: speckle tracking echocardiography. Circulation 2005;112:3149-56. http://doi.org/cq7d97

9. Hyung K, Dac S, Sang L, Su CH, Jin P, Yong K, et al. Assessment of left ventricular rotation and torsion with two-dimensional speckle tracking echocardiography. J Am Soc Echocardiogr 2007;1:45-53.

10. Anderson R, Ho S, Redmann K, Sanchez-Quintana D, Lunkenheimer P. The anatomical arrangement of the myocardial cells making up the ventricular mass. Eur J Cardiothorac Surg 2005;28:517-25. http://doi.org/d68hdp

11. Anderson R, Smerup M, Sanchez-Quintana D, Loukas M, Lunkenheimer P. The three-dimensional arrangement of the myocytes in the ventricular walls. Clin Anat 2009;22:64-76. http://doi.org/bx2xfs

12. Torrent-Guasp F. Structure and function of the heart. Rev Esp Cardiol 1998;51:91-102. http://doi.org/6tj

13. Torrent-Guasp F, Ballester M, Buckberg G, Carreras F, Flotats A, Carrio I, et al. Spatial orientation of the ventricular muscle band: physiologic contribution and surgical implications. J Thorac Cardiovasc Surg 2001,122:389-92. http://doi.org/d332kh

14. Torrent-Guasp F, Buckberg GD, Clemente C, Cox JL, Coghlan HC, Gharib M. The structure and function of the helical heart and its buttress wrapping. I. The normal macroscopic structure of the heart. Semin Thorac Cardiovasc Surg 2001;13:301-19. http://doi.org/6th

15. Mor-Avi V, Lang RM, Badano LP, Belohlavek M, Cardim NM, Derumeaux G. Current and evolving echocardiographic techniques for the quantitative evaluation of cardiac mechanics: ASE/EAE consensus statement on methodology and indications endorsed by the Japanese Society of Echocardiography. Eur J Echocardiogr 2011;12:167-205. http://doi.org/dhdvmr

16. Haugaa KH, Amlie JP, Berge KE, Leren TP, Smiseth OA, Edvardsen T. Transmural differences in myocardial contraction in long-QT syndrome. Mechanical consequences of ion channel dysfunction. Circulation 2010;122:1355-63. http://doi.org/dzj3nf

17. Simonson J, Schiller NB. Descent of the base of the left ventricle: an echocardiographic index of left ventricular function. J Am Soc Echocardiogr 1989;2:25-35. http://doi.org/5cq

18. Yingchoncharoen T, Agarwal S, Popovic ZB, Marwick TH. Normal ranges of left ventricular strain: a meta-analysis. J Am Soc Echocardiogr 2013;26:185-91. http://doi.org/bt9m

19. Kim HK, Sohn DW, Lee SE, Choi SY, Park JS, Kim YJ, et al. Assessment of left ventricular rotation and torsion with two-dimensional speckle tracking echocardiography. J Am Soc Echocardiogr 2007;20:45-53. http://doi.org/ccfcb9

20. Takahashi K, AlNaami G, Thompson R, Inage A, Mackie AS, Smallhorn JF. Normal rotational, torsion and untwisting data in c http://doi.org/c9phx4hildren, adolescents and young adults. J Am Soc Echocardiogr 2010;23:286-93.

21. Voight JU, Pedrizzetti G, Lysyansky P, Marwick TH, Houle H, Baumann R, et al. Definitions for a common standard for 2D speckle tracking echocardiography: consensus document of the EACVI/ASE/Industry Task Force to standardize deformation imaging. Eur Heart J Cardiovasc Imaging 2015;16:1-11. http://doi.org/bt9n

22. Kalam K, Otahal P, Marwick TH. Prognostic implications of global LV dysfunction: a systematic review and meta-analysis of global longitudinal strain and ejection fraction. Heart 2014;100:1673-80. http://doi.org/bt9p

23. Smiseth OA, Torp H, Opdahl A, Haugaa KH, Urheim S. Myocardial strain imaging: how useful is it in clinical decision making? Eur Heart J 2016;37:1196-207. http://doi.org/bt9q

24. Mornos C, Rusinaru D, Manolis AJ, Zacharopoulou I, Pittaras A, Ionac A. The value of a new speckle tracking index including left ventricular global longitudinal strain and torsion in patients with dilated cardiomyopathy. Hellenic J Cardiol 2011;52:299-306.

25. Trainini JC, Elencwajg B, López-Cabanillas N, Herreros J, Lago

NE, Lowenstein JA, Trainini A. Propagación de los estímulos, torsión muscular y efecto de succión cardiaca a través de la investigación electrofisiológica. En: Fundamentos de la nueva mecánica cardiaca. La bomba de succión. 1ª ed. Buenos Aires: Lumen; 2015. p. 41-67.

26. Cosín JA, Hernándiz A, Tuzón MT, Agüero J, Torrent-Guasp F. Experimental study of the so called left ventricular isovolumic relaxation phase. Rev Esp Cardiol 2009;62:392-9. http://doi.org/ccnmdc

27. Poveda F, Gil D, Martí E, Andaluz A, Ballester M, Carreras F. Helical Structure of the Cardiac Ventricular Anatomy Assessed by Diffusion Tensor Magnetic Resonance Imaging With Multiresolution Tractography. Rev Esp Cardiol 2013;66:782-90. http://doi.org/f2fnsn

28. Taber LA, Yang M, Podszus WW. Mechanics of ventricular torsion. J Biomech 1996;29:745-52. http://doi.org/bngnk7

29. Sengupta PP, Khandheria BK, Korinek J, Wang J, Jahangir A, Seward JB, et al. Apex to base dispersion in regional timing of left ventricular shortening and lengthening. J Am Coll Cardiol 2006;47:163-72. http://doi.org/c79bb9

30. Hayabuchi Y, Sakata M, Kagami S. Assessment of the helical ventricular myocardial band using standard echocardiography. Echocardiography 2015;32:310-8. http://doi.org/bt9r

31. Sengupta PP, Tajik A, Chandrasekaran K, Khandheria BK. Twist mechanics of the left ventricle. JACC Cardiovascular Imaging 2008;1:366-76. http://doi.org/dfxc4r

32. Voelkel T, Linke WA. Conformation-regulated mechanosensory control via titin domains in cardiac muscle. Pflugers Arch Eur J Physiol 2011;462:143-54. http://doi.org/dhv4jt

33. Linke WA. Sense and stretchability: the role of titin and titin-associated proteins in myocardial stress-sensing and mechanical dysfunction. Cardiovasc Res 2008;77:637-48.

34. Granzier HL, Radke MH, Peng J, Westermann D, Nelson L, Rost K. Truncation of titin's elastic PEVK region leads to cardiomyophaty with diastolic dysfunction. Circ Res 2009;105:557-64. http://doi.org/bwhtsn

35. Linke WA, Krüger M. The giant protein titin as an integrator of myocyte signaling pathways. Physiol Bethesda 2010;25:186-98. http://doi.org/d6nqvw

36. Bell SP, Nyland L, Tischler MD, McNabb M, Granzier H, LeWinter MM. Alterations in the determinants of diastolic suction during pacing tachycardia. Circ Res 2000;87:235-40. http://doi.org/bt9s

37. Ashikaga H, Criscione JC, Omens JH, Covell JW, Ingels NB Jr. Transmural left ventricular mechanics underlying torsional recoil during relaxation. Am J Physiol Heart Circ Physiol 2004;286:H640-7. http://doi.org/dsk5km